Chemical Engineering Journal 463 (2023) 142442

Contents lists available at ScienceDirect

Chemical Engineering Journal

journal homepage: www.elsevier.com/locate/cej

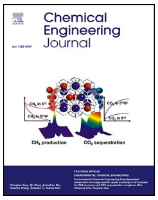

Short communication

Hybrid plasma-thermal system for methane conversion to ethylene and hydrogen

Rui Liu [a], Yingzi Hao [a], Tong Wang [a], Li Wang [b], Annemie Bogaerts [c], Hongchen Guo [a,*], Yanhui Yi [a,*]

[a] State Key Laboratory of Fine Chemicals, School of Chemical Engineering, Dalian University of Technology, Dalian 116024, Liaoning, China
[b] College of Environmental Sciences and Engineering, Dalian Maritime University, Dalian 116026, Liaoning, China
[c] Research group PLASMANT, Department of Chemistry, University of Antwerp, Universiteitsplein 1 BE-2610 Wilrijk-Antwerp, Belgium

ARTICLE INFO

Keywords:
Hybrid plasma-thermal system
Methane conversion
Ethylene
Hydrogen

ABSTRACT

By combining dielectric barrier discharge plasma and external heating, we exploit a two-stage hybrid plasma-thermal system (HPTS), i.e., a plasma stage followed by a thermal stage, for direct non-oxidative coupling of CH_4 to C_2H_4 and H_2, yielding a CH_4 conversion of ca. 17 %. In the two-stage HPTS, the plasma first converts CH_4 into C_2H_6 and C_3H_8, which in the thermal stage leads to a high C_2H_4 selectivity of ca. 63 % by pyrolysis, with H_2 selectivity of ca. 64 %.

1. Introduction

Methane conversion, a thermodynamically unfavorable process, requires high temperature and catalysts. Usually, the direct conversion into C_2 hydrocarbons has been investigated by oxidative coupling of methane (OCM) and nonoxidative coupling of methane (NOCM). Although OCM is a much better option in terms of C_2 hydrocarbons yield [1–4], a large amount of CO_x and a low efficiency of methane utilization have been obtained. For the NOCM, the overoxidation of methane and C_2 hydrocarbons can be prevented, and H_2 can be produced as a desired product instead of H_2O in OCM. Therefore, NOCM to ethylene (C_2H_4) is a promising route for CH_4 conversion, which has been achieved by thermal pyrolysis [5], catalytic methods [5–8] and plasma-based approaches [9,10].

Due to the high stability of the C–H bond in CH_4, thermal pyrolysis is typically operated at extremely high temperature, which leads to high selectivity of solid carbon (>90%), but low selectivity toward C_2 hydrocarbons (<10 %) [5,11].Recently, Bao et al. presented a Fe©SiO_2 catalyst with single atomic iron sites confined in silica matrix, being promising for CH_4 conversion to produce ethylene and aromatics. 48 % CH_4 conversion was maintained in a 60 h stability test at 1100 °C [5]. Varma et al. described that ZSM-5 zeolite supported bimetallic Pt-Bi catalysts stably and selectively convert methane (<1 %) to C_2 species with high selectivity (>90 %) at relatively moderate temperatures (600–700 °C) [11]. Dumesic et al, reported Pt and PtSn catalysts supported on SiO_2 and H-ZSM-5 for methane conversion under non-oxidative conditions at 1123 K [12]. Although the reaction temperature has been reduced by the catalytic approach, the methane non-oxidative coupling still needs to be operated at temperatures higher than 1000 °C to obtain reasonable CH_4 conversion (Table S1). Plasma has been combined with catalysts for methane non-oxidative coupling at lower temperature to obtain high CH_4 conversion, even at ambient temperature [13–15]. In plasma, the energetic electrons can effectively activate CH_4 molecule to produce abundant chemically active species such as radicals and excited species through electron-molecule collisions ($CH_4 + e \rightarrow CH_3 + H + e$; $CH_4 + e \rightarrow CH_2 + H_2 + e$). The generated active species can rapidly react with each other to produce hydrocarbons at atmospheric pressure. However, either C_2H_6 or C_2H_2 was obtained as the main product, and C_2H_4 can be obtained with satisfied selectivity only in the case of placing Pd-based hydrogenation catalysts in the post-plasma region of thermal plasma (C_2H_2 hydrogenation to C_2H_4) [16–18]. Thermodynamic calculation of CH_4 pyrolysis (Fig. S1) indicates that C_2H_4 can be produced as the dominant product at a temperature around 800 °C with CH_4 conversion lower than 10 %. Therefore, the combination of plasma chemistry and thermal pyrolysis may be a promising approach for CH_4 to C_2H_4 conversion with high selectivity and CH_4 conversion, but it has never been explored.

Herein, by combining dielectric barrier discharge (DBD) plasma and external heating, we exploited a hybrid plasma-thermal system (HPTS) for direct non-oxidative coupling of CH_4 to C_2H_4 (Fig. S2). Our results

---

* Corresponding authors.
E-mail addresses: hongchenguo@163.com (H. Guo), yiyanhui@dlut.edu.cn (Y. Yi).

https://doi.org/10.1016/j.cej.2023.142442
Received 7 January 2023; Received in revised form 18 February 2023; Accepted 12 March 2023

demonstrate that one-stage HPTS shows C_2H_4 selectivity of 80 %, but CH_4 conversion of only 2 %. However, two-stages HPTS (plasma stage followed by thermal stage) exhibits not only high C_2H_4 selectivity of ca. 63 % but also a CH_4 conversion of ca. 17 %, suggesting an excellent potential for practical conversion of CH_4 to C_2H_4 and H_2.

2. Results and discussion

Fig. 1a shows the schematic diagram of the one-stage HPTS. The DBD reactor was heated by a furnace, aiming to control the bulk reaction temperature, which was monitored by thermocouple for NOCM to C_2H_4 from 200 °C to 880 °C. Furthermore, the temperature was also recorded by a thermal infrared imager (Figs. S3–S5), which demonstrate that the temperature measured by thermocouple was nearly consistent with that of thermal infrared imager within the detection limit. Fig. 1b illustrates that, in this one-stage HPTS, higher temperatures (heated by the furnace) lead to lower specific energy input (SEI), since the electric field of the DBD was weakened by the high temperature, resulting in extremely weak discharges. This can be demonstrated by the measured discharge currents (Fig. S6b) and discharge voltages (Fig. S6a), and the discharge power calculated by Lissajous figures (Fig. S6c). The most plausible reason for the weak discharge at high temperature (>400 °C) is that the resistance of methane gas decreases with increasing temperature, and most of energy is therefore consumed by power supply with a relative high resistance [19]. The results in Fig. 1b reveal that the SEI is inversely proportional to the reaction temperature in this one-stage HPTS, and elevated temperatures lead to low SEI.

Fig. 1c depicts the CH_4 conversion and C_2H_4 selectivity as a function of reaction temperature with a initial SEI without external heating (60 or 75 kJ/L). The CH_4 conversion gradually drops, while the C_2H_4 selectivity gradually rises. Specifically, significant CH_4 conversion (10–20 %) is achieved below 400 °C with extremely low C_2H_4 selectivity (<10 %), similar to the performance of “DBD only” (without external heating), with C_2H_6 as the main product (Fig. S7). In case of high temperature (especially higher than 800 °C), the one-stage HPTS shows high C_2H_4 selectivity (50–80 %) but low CH_4 conversion (ca. 2 %). The corresponding results of H_2 selectivity are shown in Fig. S8. The CH_4 conversion is now similar to the performance of thermal pyrolysis (Fig. S9), which means that the weak discharge at high temperature in the one-stage HPTS does not help for dissociation of the C–H bond and activation of CH_4. However, the C_2H_4 selectivity is around 40 times higher than the performance of thermal pyrolysis at the same temperature (where coke is the dominant product, as shown in Fig. S9). This result suggests a complex interaction between DBD plasma and external heating in the one-stage HPTS, i.e., regulating radical species and reaction pathways, which are likely responsible for the enhancement of C_2H_4 selectivity at high temperature.

Fig. 1d illustrates the reaction performance at different SEI with fixed reaction temperature. Generally, upon increasing SEI, the CH_4 conversion rises but the C_2H_4 selectivity drops, and the highest C_2H_4 selectivity (ca. 82 %) is achieved at 880 °C with 35 kJ/L SEI (Fig. S10). Fig. 1e shows the correlation between CH_4 conversion and C_2H_4 selectivity, which demonstrates a trade-off relationship. That is, we cannot achieve high CH_4 conversion and high C_2H_4 selectivity simultaneously in one-stage HPTS. This trade-off also applies to one-stage HPTS at different flow rates, i.e., Figs. 1f and S11, in which the experimental uncertainty are shown as error bar. The intrinsic reason for this trade-off is that high SEI and high temperature cannot be realized simultaneously in this one-stage HPTS.

Implementing both high SEI and high temperature is a potential strategy to overcome the trade-off between CH_4 conversion and C_2H_4 selectivity. Thus, we designed a two-stage HPTS, i.e, plasma stage (stage 1) followed by thermal stage (stage 2), as depicted in Fig. 2a. Fig. 2b shows the performance of the two-stage HPTS with constant SEI in stage 1 (60 kJ/L) but varying temperature in stage 2. Significant and stable CH_4 conversion of ca. 17 % has been achieved at varying temperature. However, the C_2H_4 selectivity increases with rising temperature in stage 2, especially at high temperature (700–880 °C). Fig. 2c illustrates the performance of the two-stage HPTS with constant temperature (880 °C) in stage 2 but varying SEI in stage 1, and the temperature in stage 1 was enhanced by increasing SEI (Fig. S12). In this case, significant and stable C_2H_4 selectivity of ca. 60 % has been achieved at varying SEI. However, the CH_4 conversion increased with rising SEI in stage 1. These results indicate that CH_4 conversion was mainly dominated by SEI in stage 1, while C_2H_4 selectivity was mainly managed by temperature in stage 2. The influence of flow rate on methane conversion and ethylene

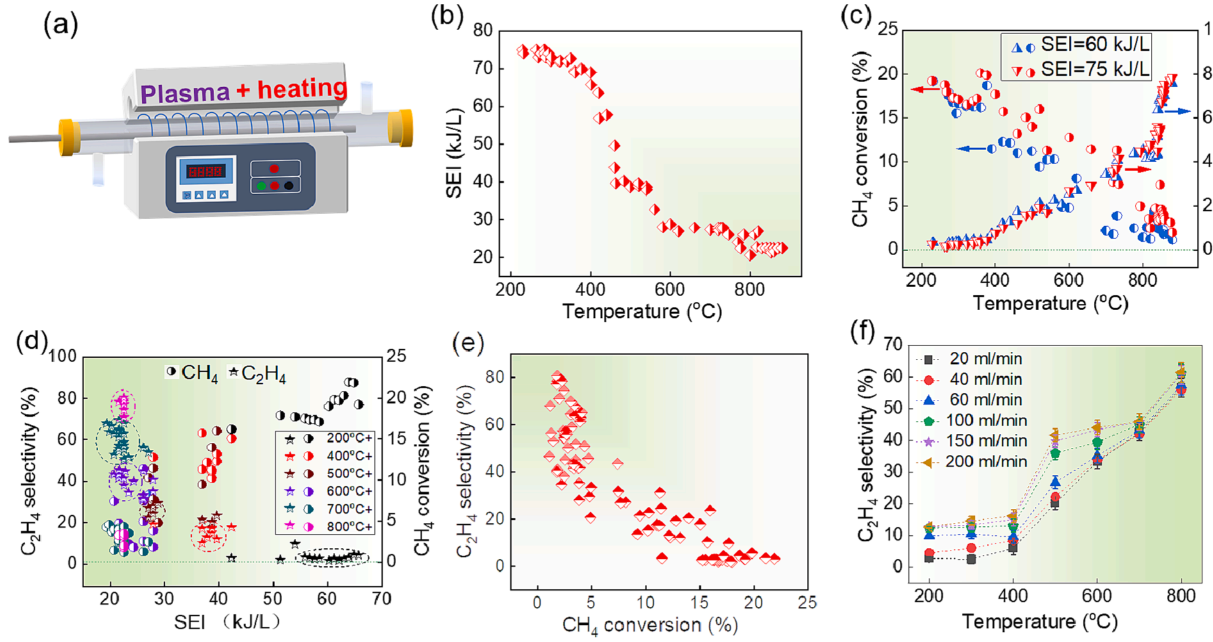

Fig. 1. Performance of the one-stage hybrid plasma-thermal system (HPTS) for methane to ethylene conversion. (a) schematic diagram of one-stage HPTS; (b) relationship of temperature and SEI; (c) CH_4 conversion and C_2H_4 selectivity as a function of temperature; (d) CH_4 conversion and C_2H_4 selectivity as a function of SEI; (e) CH_4 conversion versus C_2H_4 selectivity; (f) effect of total flow rate on C_2H_4 selectivity.

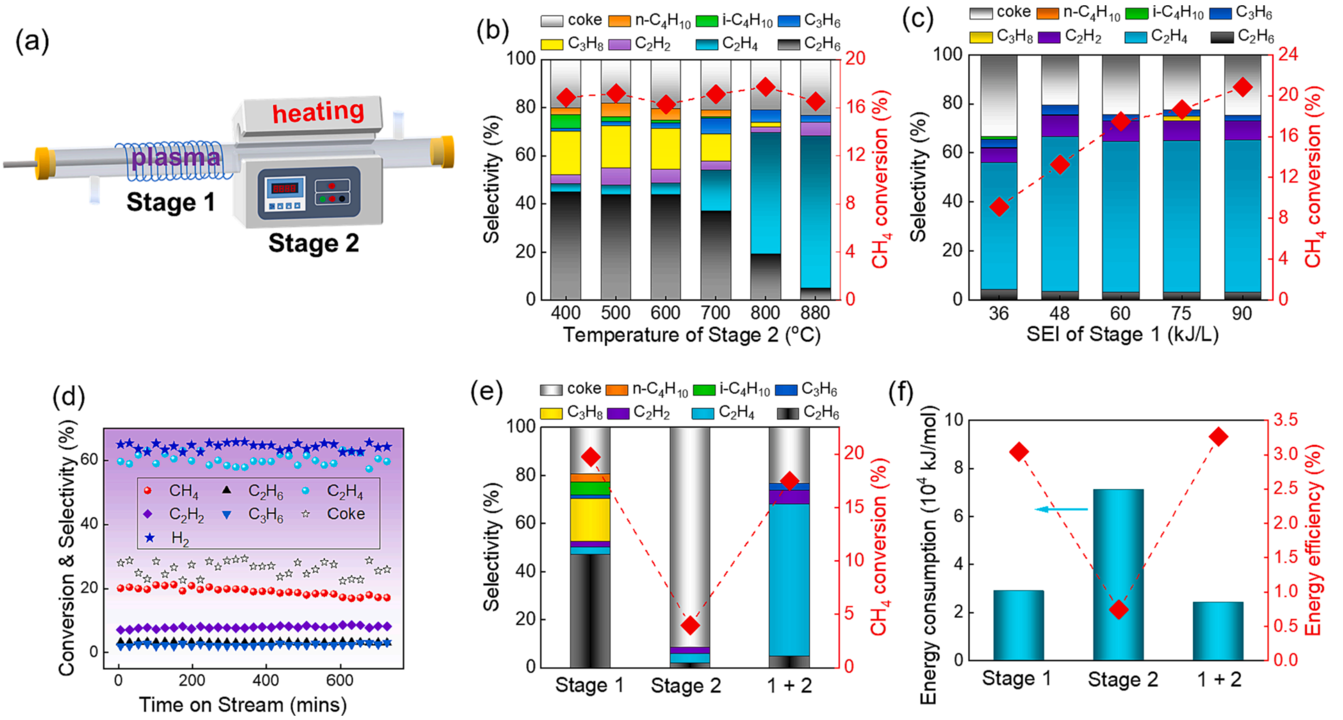

Fig. 2. Performance of the two-stage hybrid plasma-thermal system (HPTS) for methane to ethylene conversion. (a) schematic diagram of the two-stage HPTS; (b) effect of temperature in stage 2 on product selectivity and CH_4 conversion at constant SEI (60 kJ/L) in stage 1; (c) effect of SEI in stage 1 on product selectivity and CH_4 conversion at constant temperature (880 °C) in stage 2; (d) reaction stability for the two-stage HPTS for methane to ethylene at constant SEI (60 kJ/L) in stage 1 and constant temperature (880 °C) in stage 2; (e) comparison of CH_4 conversion and product selectivity between "only stage 1", "only stage 2" and "stage 1 + stage 2"; (f) comparison of energy consumption and energy efficiency of main product between "only stage 1", "only stage 2" and "stage 1 + stage 2".

selectivity in the two-stage HPTS is shown in Fig. S13, which further demonstrates that high temperature in stage 2 favors C_2H_4 production.

Fig. 2d presents the performance of the two-stage HPTS during 12 h continuous operation (at 90 kJ/L, 880 °C). A slightly decline of CH_4 conversion (Fig. S14) and stable C_2H_4 selectivity (ca. 60 %) with time on stream suggest a good performance and stability of the two-stage HPTS for methane to ethylene conversion. Correspondingly, ca. 64 % H_2 selectivity (based on H balance) has been achieved. Fig. 2e summarizes the CH_4 conversion and products distribution in case of "only stage 1" (60 kJ/L), "only stage 2" (880 °C) and "stage 1 + stage 2" (60 kJ/L, 880 °C). The case of "only stage 1" shows C_2H_6, C_3H_8 and i-C_4H_{10} as the main products with ca. 20 % CH_4 conversion. The "only stage 2" case yields coke as the main product with extremely low conversion of CH_4 (ca. 3.2 %). However, the "stage 1 + stage 2" case shows a satisfying CH_4 conversion (ca. 17 %) and an excellent C_2H_4 selectivity (ca. 63 %). The effect of distance between stage 1 and stage 2 on reaction performance has been investigated, but no obvious effects were found when the distance varied from 1 cm to 20 cm (Fig. S15). In addition, compared with "only stage 1" and "only stage 2", the "stage 1 + stage 2" shows a relatively low energy consumption (24.372 MJ/mol$_{C2H4}$) and a relative high energy efficiency (3.263 %), as indicated in Fig. 2f. Even so, they are not yet comparable to the state-of-the-art in plasma (1.2 MJ/mol$_{C2H4}$[16]) and catalytic routes (0.8 MJ/mol$_{C2H4}$[5]). This may be caused by the low methane feed flow rate (20 ml/min) and absence of catalysts in the "stage 1 + stage 2" (Fig. S15). Therefore, with the increase of methane flow rate, the energy consumption has been reduced and the energy efficiency has been improved a lot (Fig. S16b).

In terms of reactor design, separating the stage1 and stage 2 will increase the cost of setup and operations. However, the economic feasibility of the two-stage HPTS is not only dependant on the above-mentioned costs, but also on the level of scale-up and the performance indexes. Currently, the pilot scale experiment has not been carried out, and thus some commercial data are not available. Therefore, a more detail analysis of economic feasibility will be applied in our further study.

Fig. 3 depicts the temporal profiles for various *m/z* signals obtained by mass spectrometry (MS), corresponding to different species, during "only stage 1", "only stage 2" and "stage 1 + stage 2". In order to accurately record the change of products, the three stages of reactions were operated without interruption. Firstly, CH_4 conversion was operated in a DBD reactor from Plasma-on to Plasma-off, which belongs to

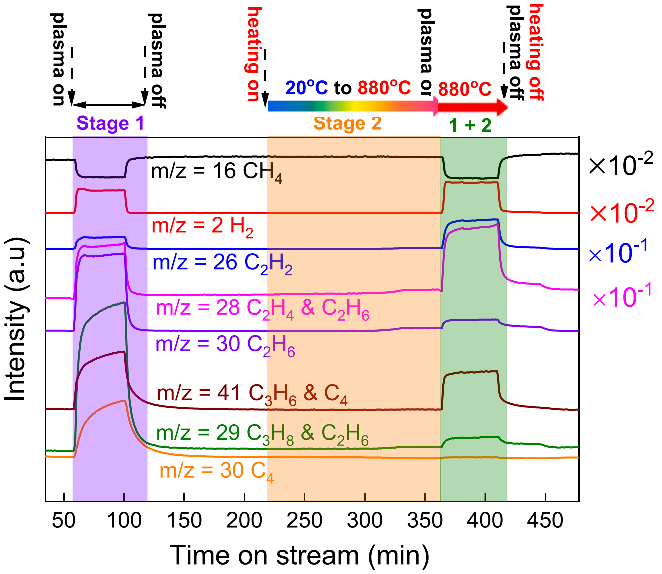

Fig. 3. Temporal profiles of MS signals with different *m/z* values (corresponding to different species), in case of "only stage 1", "only stage 2" and "stage 1 + stage 2".

Stage 1. After turning off the discharge for ca. 100 min, the heating of the furnace was then initiated until the temperature reached to 880 °C, which belongs to Stage 2. Finally, when the temperature of furnace remained at 880 °C, the discharge in the DBD reactor was turned on (plasma-on). Thus plasma activation and thermal pyrolysis were both turned on, and this belongs to "Stage 1 + Stage 2". Clearly, with the transformation from "only stage 1" to "stage 1 + stage 2", the intensity of $m/z = 28$ (which corresponds to C_2H_4 and C_2H_6) became higher, while the intensity of $m/z = 30$ (which only reflects C_2H_6) became much lower. This gives convincing evidence for the switch of the main product from C_2H_6 (only stage 1) to C_2H_4 (stage 1 + stage 2). Furthermore, compared with "only stage 1", the MS profiles also demonstrate more C_2H_2 but less C_3H_8 and C_4 in "stage 1 + stage 2". Correspondingly, in "stage 1 + stage 2", H_2 has been detected by MS with high intensity, which confirms abundant co-production of H_2. These results are consistent with the reaction performance in Fig. 2d and e.

To reveal how the two-stage HPTS converts CH_4 to C_2H_4 with high selectivity, we studied the thermal pyrolysis of C_2H_6, C_3H_8 and i-C_4H_{10}, which are the main products from stage 1. Fig. S17 shows the reaction performance for thermal pyrolysis of C_2H_6 at different temperatures. Obviously, significant C_2H_6 conversion was achieved only at temperatures higher than 700 °C, and the main product is C_2H_4. Fig. S18 illustrates similar results, but for thermal pyrolysis of C_3H_8. Again, significant C_3H_8 conversion was achieved only at temperatures higher than 700 °C, and the main products consist of C_2H_4, CH_4 and coke. Finally, the results for thermal pyrolysis of i-C_4H_{10} at different temperature, plotted in Fig. S19, also demonstrate that significant i-C_4H_{10} conversion was achieved only at temperatures higher than 600 °C, and the products consist of coke, C_2H_4, C_3H_6 and CH_4, with coke being the main product.

After analyzing the results in Figs. 2 and S16–S19, the temperature corresponding to high C_2H_4 selectivity in Fig. 2b is consistent with the temperature for efficient thermal pyrolysis of C_2H_6 and C_3H_8 to C_2H_4 in Figs. S17 and S18. These results indicate that C_2H_4 in the two-stage HPTS mainly comes from thermal pyrolysis of C_2H_6 and C_3H_8 in stage 2, while C_2H_6 and C_3H_8 originate from plasma-triggered CH_4 coupling in stage 1. However, the coke in the two-stage HPTS mainly arises from thermal pyrolysis of C_3H_8 and C_4H_{10}. Furthermore, a small drop of CH_4 conversion from "only stage 1" to "stage 1 + stage 2" in Fig. 2e is mainly caused by thermal pyrolysis of C_3H_8 and C_4H_{10}, which produces again CH_4.

A plausible reaction mechanism for CH_4 conversion to C_2H_4 and H_2 in the two-stage HPTS is proposed, as shown in Fig. 4. In the plasma (Stage 1), the activation of C–H bond in CH_4 is mainly attributed to the energetic electrons generated by dielectric barrier discharge. Firstly, the energetic electrons transfer their energy to CH_4 molecule through inelastic collisions, leading to the dissociation of C–H bond to form abundant CH_3 radical. Then C_2H_6 can be formed through recombination of CH_3 radicals, leading to the generation of the first main product (C_2H_6) in Stage 1 [20]. Meanwhile, the energetic electrons can also dissociate C_2H_6 to generated C_2H_5 radical, which can easily react with CH_3 to produce C_3H_8 as the second main product in Stage 1 [21]. Therefore, the main feed gases for stage 2 includes the unreacted CH_4 and the produced C_2H_6 and C_3H_8 from stage 1. Compared with CH_4 thermal cracking at the temperature exceeding 1000 °C, usually, pyrolysis of C_2H_6 and C_3H_8 to form C_2H_4 and C_3H_6 are much easier, and thus they can be operated at a relative lower temperature (Figs. S17 and S18). In the pyrolysis of C_2H_6 at high temperature, the related main reactions are listed in Table S4. Theoretically, both C–C bond and C–H bond can be dissociated to produce CH_3 and C_2H_5 radicals, respectively, which are the chain initiation reactions. However, in C_2H_6 molecule, the bond length of C–C bond and C–H bond are 0.1526 and 0.1101 nm, respectively. This means that C–C bond can be dissociated more easily than C–H bond. That is, the pyrolysis of C_2H_6 is mainly initiated through C–C bond breaking to produce CH_3 radicals, which induce the chain transfer reaction ($CH_3 + C_2H_6 \rightarrow CH_4 + C_2H_5$) to form C_2H_5 [22]. Subsequently, C_2H_5 decomposes to produce C_2H_4 and H. After that, H radical leads to a faster chain transfer reaction ($H + C_2H_6 \rightarrow H_2 + C_2H_5$) than CH_3 radical ($CH_3 + C_2H_6 \rightarrow CH_4 + C_2H_5$), since the energy barrier of the former is 9.7 kcal/mol while the later is 16.5 kal/mol. Therefore, $H + C_2H_6 \rightarrow H_2 + C_2H_5$ is the main reaction to consume C_2H_6 for generation of H_2 and C_2H_5, which further produce C_2H_4 through the reaction $C_2H_5 \rightarrow H + C_2H_4$ [22,23]. In the thermal cracking of C_3H_8, the related main reactions are listed in Table S5. For C_3H_8 molecule, the length of C–H bond (1.102 nm) is shorter than that of C–C bond (1.528 nm), which means that the breaking of C–C bond is easier than the C–H bond. Hence, the main reaction of the C_3H_8 cracking is $C_3H_8 \rightarrow C_2H_5 + CH_3$, but not $C_3H_8 \rightarrow C_3H_7 + H$. Subsequently, the chain reactions can be transferred by both CH_3 and C_2H_5 radicals through the reactions $CH_3 + C_3H_8 \rightarrow C_3H_7 + CH_4$ and $C_2H_5 + C_3H_8 \rightarrow C_3H_7 + C_2H_6$, respectively [22,24]. However, the energy barrier of the former (11.5 kcal/mol) is a little lower than that of the latter (12.6 kcal/mol). This means that $CH_3 + C_3H_8 \rightarrow C_3H_7 + CH_4$ is the main reaction to consume C_3H_8 for generation of CH_4 and C_3H_7 radical, which can easily decompose to produce C_2H_4 and CH_3 [22]. The CH_3 radicals will react with C_3H_8 again ($CH_3 + C_3H_8 \rightarrow C_3H_7 + CH_4$), resulting in transformation of C_3H_8 to CH_4 and C_2H_4.

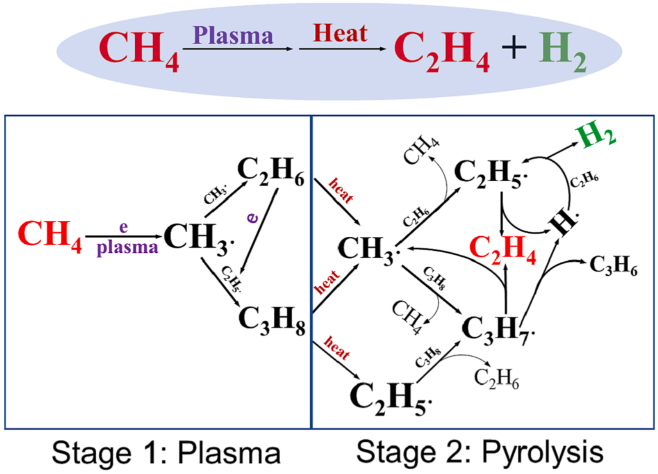

Fig. 4. The reaction mechanism of NOCM in the Two-Stage Hybrid Plasma-Thermal System.

3. Conclusion

We exploited a hybrid DBD plasma-thermal system for direct non-oxidative coupling of CH_4 to C_2H_4 and H_2. The one-stage HPTSR shows high C_2H_4 selectivity of ca. 80 %, but CH_4 conversion is only 2 %. The two-stages HPTS (plasma stage followed by thermal stage), however, exhibits not only high C_2H_4 selectivity of ca. 63 %, but also a CH_4 conversion of ca. 17 %, suggesting an excellent potential for practical conversion of CH_4 to C_2H_4 and H_2. In addition, we will design highly efficient catalysts for stage 1 to selectively produce C_2H_6, and for stage 2 to manage C_2H_6 dehydrogenation, which may lead to an innovative, efficient and practical technique for non-oxidative coupling of CH_4 to C_2H_4 and H_2 without coking. Furthermore, although the current energy efficiency is very low, we believe there is significant room for further improvement by the synergy of catalysts with plasma and the high temperature. Based on the optimized reactor design and catalysts preparation, we are quite sure that it will achieve a high conversion/yield to offset cost increase caused by separating plasma and pyrolysis stages when scaling-up the process.

Declaration of Competing Interest

The authors declare that they have no known competing financial interests or personal relationships that could have appeared to influence the work reported in this paper.

Data availability

Data will be made available on request.

Acknowledgment

This work was supported by the National Natural Science Foundation of China [22272015, 21503032], the Fundamental Research Funds for the Central Universities of China [DUT21JC40].

Appendix A. Supplementary data

Supplementary data to this article can be found online at https://doi.org/10.1016/j.cej.2023.142442.

References

[1] T.J. Marks, A.M. Arinaga, M.C. Ziegelski, Alternative oxidants for the catalytic oxidative coupling of methane, Angew. Chem. 132 (2020) 17935.

[2] I. Kim, G. Lee, H.B. Na, J.M. Ha, J.C. Jung, Selective oxygen species for the oxidative coupling of methane, Mol. Catal. 435 (2017) 13–23.

[3] A. Galadima, O. Muraza, Revisiting the oxidative coupling of methane to ethylene in the golden period of shale gas: a review, J. Ind. Eng. Chem. 37 (2016) 1–13.

[4] S. Sarsani, D. West, W. Liang, V. Balakotaiah, Autothermal oxidative coupling of methane with ambient feed temperature, Chem. Eng. J. 328 (2017) 484–496.

[5] X. Guo, G. Fang, G. Li, et al., Direct, nonoxidative conversion of methane to ethylene, aromatics, and hydrogen, Science 344 (2014) 616–619.

[6] D. Bajec, A. Kostyniuk, A. Pohar, B. Likozar, Nonoxidative methane activation, coupling, and conversion to ethane, ethylene, and hydrogen over Fe/HZSM-5, Mo/HZSM-5, and Fe–Mo/HZSM-5 catalysts in packed bed reactor, Int. J. Energy Res. 43 (2019) 6852–6868.

[7] Y. Gao, L. Neal, D. Ding, F.L. Gaffney, et al., Recent advances in intensified ethylene production-a review, ACS Catal. 9 (2019) 8592–8621.

[8] T. Zhang, Recent advances in heterogeneous catalysis for the nonoxidative conversion of methane, Chem. Sci. 21 (2021) 12529–12545.

[9] X. Zhang, L. Di, Q. Zhou, Methane conversion under cold plasma over Pd-containing ionic liquids immobilized on γ-Al_2O_3, J. Energy Chem. 22 (2013) 446–450.

[10] M. Scapinello, E. Delikonstantis, G.D. Stefanidis, The panorama of plasma-assisted non-oxidative methane reforming, Chem. Eng. Process. Process Intensif. 117 (2017) 120–140.

[11] Y. Xiao, A. Varma, Highly selective nonoxidative coupling of methane over pt-bi bimetallic catalysts, ACS Catal. 8 (2018) 2735–2740.

[12] D. Gerceker, A.H. Motagamwala, K.R. Rivera-Dones, et al., Methane conversion to ethylene and aromatics on PtSn catalysts, ACS Catal. 7 (2017) 2088–2100.

[13] L. Liu, S. Das, Z. Zhang, S. Kawi, Nonoxidative coupling of methane over ceria-supported single-atom Pt catalysts in DBD plasma, Acs Appl. Mater. Interfaces 14 (2022) 5363–5375.

[14] J. Kim, J. Jeoung, J. Jeon, et al., Effects of dielectric particles on non-oxidative coupling of methane in a dielectric barrier discharge plasma reactor, Chem. Eng. J. 377 (2019), 119896.

[15] M. Scapinello, E. Delikonstantis, G.D. Stefanidis, A study on the reaction mechanism of non-oxidative methane coupling in a nanosecond pulsed discharge reactor using isotope analysis, Chem. Eng. J. 360 (2019) 64–74.

[16] E. Delikonstantis, M. Scapinello, O. Van Geenhoven, G.D. Stefanidis, Nanosecond pulsed discharge-driven non-oxidative methane coupling in a plate-to-plate electrode configuration plasma reactor, Chem. Eng. J. 380 (2020), 122477.

[17] W. Kangjun, L.i. Xiaosong, Z.u. Aimin, A green process for high-concentration ethylene and hydrogen production from methane in a plasma-followed-by-catalyst reactor, Plasma Sci Technol. 13 (2011) 77.

[18] S. Kado, Y. Sekine, K. Urasaki, K. Okazaki, T. Nozaki, High performance methane conversion into valuable products with spark discharge at room temperature, Stud. Surf. Sci. Catal. 147 (2004) 577–582.

[19] S. Yao, A. Nakayama, E. Suzuki, Methane conversion using a high-frequency pulsed plasma: important factors, AlChE J. 47 (2001) 413–418.

[20] Y. Yang, Direct non-oxidative methane conversion bynon-thermal plasma: modeling study, Plasma Chem. Plasma Process. 23 (2003) 327–346.

[21] C. De Bie, B. Verheyde, T. Martens, J.V. Dijk, S. Paulussen, A. Bogaerts, Fluid modeling of the conversion of methane into higher hydrocarbons in an atmospheric pressure dielectric barrier discharge, Plasma Process. Polym. 8 (2011) 1033–1058.

[22] K.M. Sundaram, G.F. Froment, Modeling of thermal cracking kinetics. 3. Radical mechanisms for the pyrolysis of simple paraffins, olefins, and their mixtures, Ind. Eng. Chem. Fundam. 17 (1978) 174–182.

[23] P.D. Pacey, J.H. Purnell, Thermodynamics of Simple Polar Liquids, Ind. Eng. Chem. Fundam. 11 (1972) 233–239.

[24] O.A. Stadnichenko, L.F. Nurislamova, N.S. Masyuk, V.I.N. Snytnikov, V. N. Snytnikov, Radical mechanism for the gas-phase thermal decomposition of propane, Reac. Kinet. Mech. Cat. 123 (2018) 607–624.